HHS Public Access

Author manuscript

*Cell*. Author manuscript; available in PMC 2017 February 25.

Published in final edited form as:

*Cell*. 2016 February 25; 164(5): 884–895. doi:10.1016/j.cell.2016.02.006.

# EGLN1 Inhibition and Rerouting of α-Ketoglutarate Suffice for Remote Ischemic Protection

**Benjamin A. Olenchock**[1,*], **Javid Moslehi**[2,*], **Alan H. Baik**[3], **Shawn M. Davidson**[4], **Jeremy Williams**[1], **William J. Gibson**[5], **Abhishek A. Chakraborty**[9], **Kerry A. Pierce**[5], **Christine M. Miller**[6], **Eric A. Hanse**[7], **Ameeta Kelekar**[7], **Lucas B. Sullivan**[4], **Amy J. Wagers**[6,8], **Clary B. Clish**[5], **Matthew G. Vander Heiden**[4,9], and **William G. Kaelin Jr.**[9,10]

[1]Division of Cardiovascular Medicine, Department of Medicine, The Brigham and Women's Hospital, Harvard Medical School, Boston, MA 02115, USA

[2]Division of Cardiovascular Medicine, Department of Medicine, Vanderbilt School of Medicine, Nashville, TN 37235, USA

[3]University of California, San Francisco, San Francisco, CA 94117, USA

[4]Koch Institute for Integrative Cancer Research at Massachusetts Institute of Technology, Cambridge, MA 02139, USA

[5]Metabolite Profiling Platform, Broad Institute; Cambridge, MA 02142, USA

[6]Harvard Department of Stem Cell and Regenerative Biology, Harvard University, Cambridge, MA 02138, USA and Joslin Diabetes Center, Boston, MA 02215, USA

[7]Department of Laboratory Medicine and Pathology and Masonic Cancer Center, University of Minnesota, Minneapolis, MN, 55455, USA

[8]Joslin Diabetes Center, Boston, MA 02215, USA

[9]Department of Medical Oncology, Dana-Farber Cancer Institute; Boston, MA 02215; USA

[10]Howard Hughes Medical Institute, Chevy Chase, MD 20815; USA

## SUMMARY

Ischemic preconditioning is the phenomenon whereby brief periods of sublethal ischemia protect against a subsequent, more prolonged, ischemic insult. In remote ischemic preconditioning (RIPC), ischemia to one organ protects others organs at a distance. We created mouse models to ask if inhibition of the alpha-ketoglutarate (αKG)-dependent dioxygenase Egln1, which senses

Correspondence: william_kaelin@dfci.harvard.edu.

*These authors contributed equally to this work.

**AUTHOR CONTRIBUTIONS**

B.A.O., S.M.D. and J.W. did the metabolism experiments and GC-MS. J.M. and A.H.B. did the mouse physiology experiments. A.W. designed parbiosis experiments, and C.M. did the parabiosis surgeries. W.J.G. performed computational analysis. E.A.H. and A.K. supplied U-$^{13}$C-dimethy-alpha-ketoglutarate. K.A.P. and C.B.C. performed and analyzed LC-MS analyses. B.A.O., J.M., M.G.V.H. and W.G.K. designed the experiments. B.A.O. and W.G.K. wrote the manuscript.

oxygen and regulates the HIF transcription factor, could suffice to mediate local and remote ischemic preconditioning. Using somatic gene deletion and a pharmacological inhibitor, we found that inhibiting Egln1 systemically or in skeletal muscles protects mice against myocardial ischemia-reperfusion (I/R) injury. Parabiosis experiments confirmed that RIPC in this latter model was mediated by a secreted factor. Egln1 loss causes accumulation of circulating αKG, which drives hepatic production and secretion of kynurenic acid (KYNA) that is necessary and sufficient to mediate cardiac ischemic protection in this setting.

## Graphical Abstract

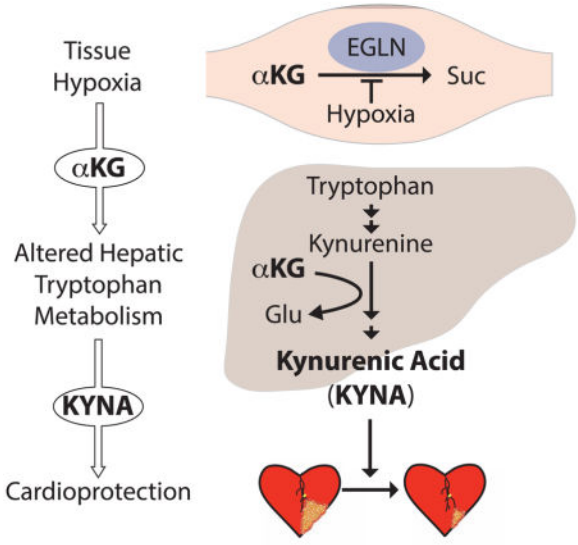


## INTRODUCTION

Brief periods of sublethal ischemia can protect tissues from a subsequent, more severe, ischemia-reperfusion (I/R) insult. This phenomenon of ‘ischemic preconditioning’ was first observed in experimental models of myocardial infarction (MI) (Murry et al., 1986) and later in coronary heart disease patients (Kloner et al., 1995). Patients who have angina (ischemic cardiac chest pain) within 48 hours before a MI have better outcomes than patients who do not experience preceding angina. Subsequent studies with animals showed that ischemia in one coronary artery territory could protect myocardium perfused by another coronary artery (Przyklenk et al., 1993), and that coronary effluent from an ischemic heart can protect a naive acceptor heart *ex vivo* (Dickson et al., 1999). Remarkably, ischemia to a non-cardiac organ also protects the heart at a distance (Gho et al., 1996). Some, but not all, human clinical trials showed that inducing arm ischemia improved outcomes after coronary artery interventions associated with iatrogenic cardiac ischemia (Davies et al., 2013) (Hausenloy et al., 2015; Meybohm et al., 2015; Thielmann et al., 2013). Many RIPC mechanisms have been proposed, including both humoral and neural mechanisms (Przyklenk, 2013).

The HIF transcription factor, which consists of a labile α subunit and a stable β subunit, accumulates during hypoxia and activates genes whose products promote cellular survival

under ischemic conditions. The HIFα subunit is regulated through prolyl hydroxylation by α-ketoglutarate (αKG) dependent-dioxygenases known as EGLNs (also called PHDs). Of the 3 EGLN paralogs, EGLN1 is the primary regulator of HIFα (Kaelin and Ratcliffe, 2008). Hydroxylated HIFα is bound by the von Hippel Lindau (VHL) tumor suppressor protein, which marks HIFα for degradation. EGLNs require $O_2$, and HIFα hydroxylation is thus impaired when $O_2$ is limited, allowing HIFα accumulation. In sum, EGLNs act as '$O_2$ sensors' in metazoans and coordinate cellular responses that promote adaptation to hypoxia and ischemia (Kaelin and Ratcliffe, 2008).

Cardiac-specific *Egln1* inactivation during late embryogenesis protects adult mice from MI after permanent coronary artery occlusion (Hölscher et al., 2011). Similarly, mice homozygous for a hypomorphic *Egln1* allele have less myocardial damage after I/R than *Egln1* +/+ mice (Hyvärinen et al., 2010). Conversely, both local and remote preconditioning are attenuated in *Hif1α* +/− mice (Cai et al., 2007; 2013). Collectively, these results support that HIF protects the heart during acute MI. However, chronic manipulation of HIF causes adaptations, such as increased angiogenesis and decreased mitochondria, that might be irrelevant to therapies aimed at acutely modulating the HIF response in patients with acute myocardial ischemia and impending MI (Huang et al., 2008). Moreover, a recent report challenged the conclusion that HIF1α is required for RIPC (Kalakech et al., 2013).

Others have acutely inactivated Egln at the time of experimental MI. The pharmacological prolyl hydroxylase inhibitors, FG0041, GSK360, and 2-(1-chloro-4-hydroxyisoquinoline-3-carboxamido) acetate (ICA) have been shown to be cardioprotective in rodents (Bao et al., 2010; Nwogu et al., 2001; Vogler et al., 2015). However, these drugs might inhibit other α-ketoglutarate (αKG)-dependent dioxygenases in addition to the Egln. Indeed FG0041 was initially tested in this setting because it inhibits the collagen prolyl hydroxylases and only later shown to inhibit the Egln (Nwogu et al., 2001). Several groups reported ischemic cardioprotection in mice after intraperitoneal (i.p.) (Natarajan et al., 2006) or intraventricular (Eckle et al., 2008) injection of naked *Egln1* siRNAs or intramyocardial injection of a plasmid encoding an *Egln1* shRNA (Huang et al., 2008). Although these interventions reportedly induced HIF, the bioavailability of siRNAs and plasmids delivered in this way is suspect. Moreover, it was later revealed that the Egln1 siRNA used in one of these studies targeted a collagen prolyl hydroxylase rather than Egln1, raising questions about specificity (Natarajan et al., 2006). Finally, a recent study reported that intramuscular injection of an adenovirus encoding HIF1α acutely protected the heart at a distance (Cai et al., 2013).

## RESULTS

### Chronic Egln1 Inactivation in Cardiomyocytes Protects Against I/R Injury

We used genetic and pharmacological tools to probe the role of Egln1 and HIF in local and remote ischemic preconditioning. Adult mice in which *Egln1* has been deleted in the heart at ~E12.5 experience less myocardial damage after permanent occlusion of the left anterior descending (LAD) coronary artery than do control mice, implying that Egln1 plays a cardiac-intrinsic role in cardioprotection (Hölscher et al., 2011). To ask whether this is also true in an ischemia-reperfusion (I/R) model, which more closely mimics myocardial injury during clinical MI, we crossed mice with a conditional (floxed or "F") *Egln1* allele with a

mouse strain expressing Cre recombinase under the control of the cardiac-specific alpha myosin heavy chain (MHC) promoter (Agah et al., 1997). We confirmed inactivation of *Egln1* in the heart, but not skeletal muscle, liver and kidney, in $Egln1^{F/F}$;*MHC-Cre* mice (Figure S1A). As expected, heart-specific *Egln1* inactivation induced HIF target genes (Figure S1B). Moreover, cardiac-specific *Egln1* inactivation was cardioprotective in mice subjected to cardiac I/R injury (Figure S1C) and in isolated hearts in a Langendorff model of global myocardial ischemia, as reflected by a faster recovery (lowering) of end-diastolic pressures compared to control mice (Figure S1D). Therefore chronic Egln1 inactivation confers cardiac-intrinsic protection against both permanent and transient cardiac ischemia.

## Acute Systemic Egln1 Inactivation Protects the Heart Against I/R Injury

We next tested an Egln inhibitor, FG-4497 (Fibrogen; (Laitala et al., 2012; Robinson et al., 2008)), in the same cardiac I/R injury models. We first confirmed that FG-4497 induced HIF1α in HL-1 cardiomyocytes (Figure 1A) and inhibited Egln *in vivo* as determined by imaging mice that ubiquitously express a HIF1α-luciferase fusion reporter (Safran et al., 2006). (Figure 1B). Notably, FG-4497 stabilized HIF1α and induced HIF target genes in the heart (Figure 1C and 1D). Pretreatment with FG-4497 decreased cardiac injury after I/R in the Langendorff model (Figure 1E) and decreased MI size in mice subjected to LAD occlusion/release *in vivo* by ~30% (Figure 1F). Importantly from a clinical perspective, FG-4497 treatment at the time of reperfusion also substantially reduced infarct sizes (Figure 1G).

Next we used $Egln1^{F/F}$;$Cre^{ER}$ mice that ubiquituously express a tamoxifen (TAM)-activatable $Cre^{ER}$ fusion protein (Minamishima et al., 2008). Giving such mice TAM for three days significantly decreased *Egln1* mRNA levels in the heart, kidney and skeletal muscle compared to TAM-treated $Egln1^{+/+}$;$Cre^{ER}$ mice (Figure 2A), and induced HIF1α protein (Figure 1C) and HIF-responsive mRNAs in the heart (Figure 2B). Acute, systemic, inactivation of Egln1 decreased myocardial injury in the Langendorff I/R model (Figure 2C) and decreased MI size in mice subjected to cardiac I/R *in vivo* compared to TAM-treated $Egln1^{+/+}$;$Cre^{ER}$ control mice (Figure 2D). Consistent with Egln1 being the relevant target of FG-4497, the effects of the combined *Egln1* gene deletion and pharmacologic Egln inhibition were subadditive (Figure 2E). Therefore acute systemic Egln1 inactivation protects against cardiac I/R injury.

## Skeletal Muscle *Egln1* Deletion Confers Remote Cardiac Ischemic Protection

Protection against cardiac I/R injury after systemic *Egln1* loss could reflect a cell-autonomous effect in cardiomyocytes, a non-cell autonomous “remote” effect on the heart, or both. To explore non-cell autonomous effects, we made mice in which *Egln1* could be conditionally inactivated specifically in skeletal muscle. $Egln1^{F/F}$ and $Egln1^{+/+}$ mice were crossed with mice expressing a TAM-dependent $Cre^{ER}$ transgene driven by a skeletal muscle-specific promoter (human alpha actin; *HSA-Cre-*$ER^{T2}$) (Schuler et al., 2005). $Egln1^{F/F}$;*HSA-Cre-*$ER^{T2}$ and $Egln1^{+/+}$;*HSA-Cre-*$ER^{T2}$ mice were given TAM or vehicle for five days and sacrificed 5 days later. *Egln1* was recombined in multiple skeletal muscle groups of TAM-treated $Egln1^{F/F}$;*HSA-Cre-*$ER^{T2}$ mice, but not in other tissues tested, such as the heart and liver (Figure S2A). *Egln1* deletion decreased skeletal muscle *Egln1* mRNA

and protein levels (Figure 3A and 3B). Importantly, hearts from TAM-treated *Egln1*$^{F/F}$;*HSA-Cre-ER*$^{T2}$ mice did not exhibit decreased *Egln1* mRNA (Figure 3A), decreased Egln1 protein (Figure S2B), increased HIF1α protein (Figure S2C), or increased HIF-responsive mRNAs (Figure S2D and S2E).

We next asked whether *Egln1* deletion in the skeletal muscle can protect the heart at a distance. TAM-treated *Egln1*$^{F/F}$;*HSA-Cre-ER*$^{T2}$ and *Egln1*$^{+/+}$;*HSA-Cre-ER*$^{T2}$ mice were subjected to *in vivo* cardiac I/R injury. Deletion of *Egln1* in the skeletal muscle reduced MI size after cardiac I/R injury by ~40% (Figure 3C). HIF induces nitric oxide synthase in certain cell types (Coulet et al., 2003), which might protect the heart by increasing nitric oxide production and decreasing afterload. We did not, however, detect differences in blood pressures between TAM-treated *Egln1*$^{F/F}$;*HSA-Cre-ER*$^{T2}$ and *Egln1*$^{+/+}$;*HSA-Cre-ER*$^{T2}$ mice (Figure S2F), nor alterations of blood nitrite levels (Figure S2G) (Coulet et al., 2003). These data show that Egln1 inactivation in skeletal muscles confers remote ischemic cardioprotection.

## Remote Ischemic Protection by Skeletal Muscle *Egln1* Gene Deletion is Mediated by a Humoral Factor

It is debated whether an intact peripheral nervous system, a soluble humoral factor, or both are required for RIPC (Przyklenk, 2013). To ask whether a humoral factor mediates RIPC in mice with skeletal muscle-specific *Egln1* deletion, we performed a parabiosis experiment. Parabiosis pairings were made between wild-type (WT) mice ("recipient" partner) and either *Egln1*$^{F/F}$;*HSA-Cre-ER*$^{T2}$ or *Egln1*$^{+/+}$;*HSA-Cre-ER*$^{T2}$ mice ("donor" partner). The donor mice were given TAM for 5 days, and 5 days later the recipient mice were subjected to cardiac I/R injury. Evan's blue dye injected 2 days later confirmed shared circulation in both types of pairings (Figure 3E). Genotyping confirmed *Egln1* deletion specifically in the skeletal muscle of TAM-treated *Egln1*$^{F/F}$;*HSA-Cre-ER*$^{T2}$ donor mice (Figure 3D). Recipient parabiosis partners of *Egln1*$^{F/F}$;*HSA-Cre-ER*$^{T2}$ mice had ~30% smaller MIs than did recipient partners of *Egln1*$^{+/+}$;*HSA-Cre-ER*$^{T2}$ mice (Figure 3F). These data argue that a humoral factor mediates RIPC after *Egln1* deletion in skeletal muscle.

## Egln1 Inactivation Alters Circulating Tryptophan Metabolites

To look for circulating cardioprotective factors that were upregulated after skeletal muscle deletion of *Egln1*, we profiled serum cytokines in TAM-treated *Egln1*$^{F/F}$;*HSA-Cre-ER*$^{T2}$ and *Egln1*$^{+/+}$;*HSA-Cre-ER*$^{T2}$ mice. None of the 144 cytokines profiled were upregulated >10% after *Egln1* loss in skeletal muscle (Figure S3A). In particular, we did not detect changes in the levels of IL-10 and EPO, which have previously been implicated in RIPC (Cai et al., 2013; 2003) (Figure S3B). In addition, pretreatment with a JAK1/2 inhibitor (Ruxolitinib), which blocks signaling by many cytokine receptors, did not abrogate RIPC in our model (Figure S3C). We concluded that the humoral mediator of RIPC in our model was not one of the cytokines examined or a cytokine that signals through JAK1/2.

Next, we analyzed gene expression profiles in skeletal muscles from TAM-treated *Egln1*$^{F/F}$;*HSA-Cre-ER*$^{T2}$ and *Egln1*$^{+/+}$;*HSA-Cre-ER*$^{T2}$ mice, and compared differentially regulated genes to a published list of genes predicted to encode secreted proteins (Wu et al.,

2010). 41 genes were differentially expressed in the skeletal muscles from TAM-treated *Egln1$^{F/F}$;HSA-Cre-ER$^{T2}$* (q<0.1), 7 of which encode proteins predicted to be secreted (Natarajan et al., 2006; Wu et al., 2010). Real-time PCR confirmed up-regulation of 2 of these 7 mRNAs, *PLAC9* and *LYPD1* (Figure S3D). Relatively little is known of the biologic function of *PLAC9* and neither gene, to our knowledge, is known to encode circulating polypeptides.

We next looked for a potential small molecule mediator(s) of cardioprotection. Blood was collected from TAM-treated *Egln1$^{F/F}$;HSA-Cre-ER$^{T2}$* and *Egln1$^{+/+}$;HSA-Cre-ER$^{T2}$* mice, and serum and plasma metabolites were profiled by LC-MS. Among the metabolites with statistically significant differences were various tryptophan (TRP)-related metabolites (Figure 4A). To narrow the list of possible mediators of remote cardiac I/R protection, we did an orthogonal experiment by profiling selected serum metabolites in WT mice given FG-4497 or vehicle (Figure 4B). We hypothesized that the cardioprotective mediator(s) would be induced by both genetic and pharmacological Egln1 inhibition, that systemic Egln1 inhibition might alter levels of the metabolite(s) of interest to an even greater extent than skeletal muscle deletion of *Egln1*, and that the cardioprotective metabolite(s) would be induced rapidly by FG-4497 since FG-4497 protected hearts even when administered *after* ischemic injury (Figure 1G). Strikingly, we observed significant changes in circulating TRP metabolites 10 minutes after FG-4497 treatment (Figure 4B).

## The Tryptophan Metabolite Kynurenic Acid Mediates Remote Ischemic Protection after Egln1 Inactivation

We focused on the TRP metabolite kynurenic acid (KYNA) as a possible cardioprotective agent because KYNA is tissue protective in models of cerebral and renal injury (Germano et al., 1987; Pundir et al., 2013; Zwilling et al., 2011). KYNA production from TRP is regulated by a rate-limiting pyrolase TRP dioxygenase (TDO) in the liver or indoleamine 2,3 dioxygenase (IDO) in peripheral tissues, as well as by αKG-dependent transamination performed by kynurenine transaminases (KAT; Figure 4C) (Agudelo et al., 2014). We confirmed that the mass spectrometry ion counts we obtained for serum KYNA and αKG in mice were in the linear ranges for their respective assays and consistent with serum concentrations of ~5 μM and ~50 μM, respectively in untreated WT mice (Figure S3E–F).

To ask whether KYNA was needed for cardiac I/R protection after skeletal muscle *Egln1* deletion, TAM-treated *Egln1$^{F/F}$;HSA-Cre-ER$^{T2}$* and *Egln1$^{+/+}$;HSA-Cre-ER$^{T2}$* controls were given 1-methyl tryptophan (1MT), a reversible inhibitor of both TDO and IDO, before cardiac I/R injury. 1-MT partially abrogated the protection caused by skeletal muscle deletion of *Egln1*, but did not affect MI sizes in control animals (Figure 4D). Conversely, pretreatment of WT mice with KYNA (Andiné et al., 1988) or the KYNA mimetic L689,560 decreased MI size compared to vehicle-treated mice (Figure 4E and 4F). Cardioprotection by KYNA appeared to be heart-autonomous, as addition of KYNA to the perfusate of isolated hearts improved ischemia tolerance in Langendorff assays (Figure 4G). These data argue that KYNA is necessary and sufficient for remote cardiac ischemic protection following Egln1 inhibition.

### Egln1 Inhibition Generates KYNA via Altered Systemic αKG Metabolism

KYNA was not induced by inactivating Egln1 in various cell culture models (Figure S4A) and mRNAs linked to TRP metabolism were not induced in skeletal muscle after inactivating Egln1 (Figure S4B), suggesting that the increased KYNA observed after Egln1 inactivation in skeletal muscle *in vivo* was indirect and non-cell autonomous. In order to determine the organ(s) producing KYNA in our model, mice were infused with U-$^{13}$C-TRP and then given FG-4497 (Figure S4C). Newly formed U-$^{13}$C-KYNA was detected in the serum, liver, kidneys, and lung, but not in skeletal muscle (Figure 5A). We concluded that KYNA is made by a tissue other than muscle after Egln1 inactivation in skeletal muscle.

Hepatic KYNA production was intriguing because the TRP metabolites n-methylnicotinamide (NMN) and niacinamide (NAM), which can be made only by the liver and the kidney, were among the serum metabolites downregulated by skeletal muscle *Egln1* loss (Figure 4A). Moreover, our U-$^{13}$C-TRP studies confirmed conversion of TRP to NMN and NAM in the liver and not the kidney (data not shown). Up-regulation of circulating KYNA combined with down-regulation of NMN and NAM suggested altered hepatic TRP metabolism after Egln inhibition (Figure 4C).

How might targeting Egln—via systemic FG-4497 administration or skeletal muscle deletion of *Egln1*—regulate hepatic TRP metabolism? We found no differences in mRNA levels for KYNA pathway enzymes in the liver (Figure S4D) of TAM-treated *Egln1$^{F/F}$;HSA-Cre-ER$^{T2}$* mice compared to control mice. Moreover, serum KYNA was increased 10 minutes after systemic FG-4497 administration (Figure 4B). These two observations suggested that control of KYNA by Egln1 in this model did not involve transcriptional changes in the liver.

KYNA production is regulated by KATs (Agudelo et al., 2014) which, like Egln1, require αKG as a co-substrate. αKG accumulates under hypoxic conditions and after pVHL loss (with consequent HIF stabilization) (Metallo et al., 2012; Wise et al., 2011), suggesting that αKG might link Egln1 inactivation to KYNA production. Indeed, αKG levels were elevated in the serum (Figure 4A), skeletal muscle, and liver in TAM-treated *Egln1$^{F/F}$;HSA-Cre-ER$^{T2}$* mice compared to control mice (Figure 5B) and in the livers of mice given FG-4497 compared to vehicle (Figure 5C). Systemic administration of αKG, like FG-4497, rapidly (10 minutes) increased circulating and hepatic KYNA levels (Figure 5D). Importantly, systemic αKG administration also protected hearts subjected to I/R injury *in vivo* (Figure 5E) and *ex vivo* in the Langendorff model (Figure 5F). In notable contrast to KYNA, however, αKG did not provide I/R protection when added directly to the perfusate in the Langendorff model (Figure 5F), consistent with the idea that αKG protects *in vivo* by increasing hepatic KYNA production.

### HIF-independent Regulation of αKG Metabolism by Egln1

In cell culture models, hypoxia and FG-4497 both increased αKG levels (Figure 6A–B). This was true whether αKG levels were normalized to cell number, or to the dioxygenase product succinate (αKG/Suc ratio) or to the transamination partner glutamate (αKG/Glu ratio). FG-4497 had minimal effect on αKG in cells Egln1−/− cells, supporting an on-target

drug effect (Figure S5A). The rapid induction of αKG (Figure 5C) and KYNA (Figure 4B) after Egln1 inactivation *in vivo* suggested that the accumulation of αKG in this setting does not require the canonical Egln1 target HIFα and transcriptional induction of HIF target genes. Consistent with this view, FG-4497 and hypoxia increased the αKG/Glu ratio in Hepa-1c1c7 cells that lack the requisite HIFα transcriptional partner ARNT (Figure 6C) and, accordingly, cannot activate a HIF-responsive luciferase reporter after Egln inhibition (Figure 6D) despite HIF1α stabilization (Figure 6E). Taken together, our data suggest that Egln inhibition in skeletal muscle—in a manner independent of HIF transcriptional activity—increases circulating and hepatic αKG, which drives the production of the cardioprotective metabolite KYNA.

We hypothesized that Egln1 inhibition increases αKG levels as a direct or indirect consequence of altered decarboxylation of its co-substrate, αKG. Egln1 is highly active, with a maximum rate of αKG decarboxylation of 45 mol/mol Egln1/min (Hirsilä et al., 2005). We estimate that 1 gram of skeletal muscle protein contains approximately 6.11 picomoles of Egln1, which based on the above rate, could decarboxylate 275 picomoles αKG /minute (Figure S5B–F). As a point of reference, this flux is ~0.5% of the skeletal muscle glycolytic rate (Kummitha et al., 2014).

To assess this predicted high rate of flux further, we traced the conversion of esterified, $^{13}$C-αKG to succinate over time in cells. $^{13}$C-αKG was rapidly converted to $^{13}$C-succinate in both WT (Figure 6F) and Cytochrome B mutant 143B cybrid cells (Figure S5G–H). This conversion was enhanced by ectopic expression of WT, but not catalytically-defective, EGLN1 (Ladroue et al., 2008), and was decreased by 10-minute pretreatment with FG-4497. These effects of manipulating EGLN1 were not due to indirect changes in $O_2$ consumption because Cytochrome B mutant cells lack an intact electron chain and are respiration defective (Sullivan et al., 2015). These experiments yielded an estimated rate of αKG decarboxylation by EGLN1 of ~200 picomoles/min/g of tissue (Figure S5I). The actual rate might be higher in tissues with high metabolic rates such as the heart, muscle and liver. Collectively, these findings support a high rate of EGLN1-dependent conversion of αKG to succinate and implicate EGLN1 in the direct control of central carbon metabolism.

## DISCUSSION

Cardiovascular diseases such as MI and stroke are the leading cause of death worldwide. Our findings confirm and extend earlier claims that chronic Egln1 inactivation, as well as chronic HIF stabilization, protects the heart against I/R injury (Cai et al., 2007; Hyvärinen et al., 2010) and permanent ligation injury (Bao et al., 2010; Nwogu et al., 2001). However, prolonged HIF activation can ultimately cause deleterious cardiac effects, culminating in dilated cardiomyopathy (Bekeredjian et al., 2010; Huang et al., 2004; Moslehi et al., 2010). Moreover, these preclinical models of chronic HIF activation do not necessarily address the utility of acutely inactivating Egln1 in the pre or peri-infarct setting. Using both a conditional *Egln1* allele and a small molecule Egln1 inhibitor we found that acute Egln inactivation protects the heart against I/R injury. Importantly, the use of a pharmacological inhibitor, in contrast to the genetic model, allowed us to model drug treatment at the time of injury, where we again observed significant protection. Nonetheless, EglN1 inhibition might

ultimately be most effective when used prophylactically, such as in the setting of unstable angina or elective cardiac surgery, which are associated with a high risk of an ischemic insult.

The cardioprotective effects observed after acute, systemic, Egln1 inactivation are likely to involve both cardiomyocyte-intrinsic HIF-dependent effects as well as remote effects. Since Egln1 is ubiquitously expressed and would predictably be inhibited by tissue ischemia, such remote effects could potentially underlie RIPC. Indeed, we found that acute, genetic ablation of *Egln1* in skeletal muscles protects the heart at a distance.

We discovered that acute Egln1 inhibition leads to rapid, HIF-independent, systemic induction of αKG, which drives hepatic transamination of the TRP metabolite kynurenine (KYN) to produce KYNA, presumably by stimulating one of several known αKG-dependent KATs. Notably, perivenous hepatocytes are able to utilize circulating αKG to support transamination reactions (Stoll and Hüssinger, 1989). KYNA was previously shown to be tissue protective in models of cerebral and renal ischemia (Andiné et al., 1988; Germano et al., 1987; Pundir et al., 2013). We observed that KYNA is cardioprotective both *in vivo* and *ex vivo*, and is both necessary and sufficient for remote cardiac protection after skeletal muscle inactivation of Egln1. Although KYNA is critical in our model, additional humoral and neural factors might also contribute to RIPC.

Notably, KYNA is elevated in survivors of cardiac arrest—a condition of systemic ischemia—in both animal models and in humans (Ristagno et al., 2013). Also, the KYNA precursor, KYN, is induced in hypoxic cells as part of a ‘catabolic signature’ of hypoxia (Frezza et al., 2011). Additionally the downstream kynurenine pathway metabolite anthranilate is one of the few metabolites elevated for sustained periods after MI, suggesting changes in TRP metabolism during cardiac ischemia (Lewis et al., 2008). These observations underscore a potential role of TRP metabolism in the response to ischemia.

Our data suggest that acute inactivation of Egln1, which utilizes αKG as a co-substrate, causes the rapid accumulation of αKG. The rate of αKG decarboxylation by Egln1 is predicted to be high because of the rapid turnover of its hydroxylation targets, the HIFα proteins. Biochemical experiments also suggest that the EglNs decarboxylate αKG in an uncoupled reaction in the absence of a polypeptide substrate so long as adequate reducing equivalents are available (Hirsilä et al., 2005), although the relative importance of coupled and uncoupled αKG decarboxylation by the Egln*s in vivo* is unknown. Nonetheless, our experiments with $^{13}$C-αKG are consistent with a very high rate of αKG metabolism by Egln1. Although it is difficult to predict changes in metabolite pool sizes from changes in flux rates, the rapid induction of αKG after Egln1 inhibition is likely due, at least in part, to the abrupt decrease in αKG utilization by Egln1. Notably, acutely inhibiting an αKG flux of nanomoles per minute on a whole mouse basis could theoretically alter serum αKG concentrations in the physiological (μM) range. It is also possible that Egln1 has a non-canonical substrate that acutely influences αKG pool sizes, or that changes in Egln1 metabolic flux indirectly alter other processes that ultimately impact αKG pool sizes. Finally, decreased αKG uptake by tissues after Egln1 loss might contribute to redistribution of αKG in vivo.

KYNA is an agonist for the aryl hydrocarbon receptor, where it can affect transcription, and a ligand for various receptors including NMDA receptors, neuronal cholinergic α7 nicotine receptors, and the orphan G-coupled receptor GPR35. Interestingly, GPR35 is a HIF target that is induced during cardiac remodeling (Ronkainen et al., 2014). Clearly additional studies are required to determine how KYNA protects the heart.

The mediator(s) of RIPC have been sought for more than 20 years, in hopes they could be used to treat cardiovascular diseases. Two recent large, randomized, studies, however, did not find a benefit of RIPC in patients undergoing cardiac surgery (Hausenloy et al., 2015; Meybohm et al., 2015). Our findings suggest that the efficacy of RIPC could be influenced by many variables including duration and magnitude of ischemia, skeletal muscle mass, hepatic function, and concurrent medications, including drugs metabolized in the liver, such as anesthetics. With respect to the latter, these two studies required and allowed, respectively, the use of propofol, which has been suggested to block RIPC (Kottenberg et al., 2012; 2014). Direct administration of KYNA might be a more robust way to protect tissues such as the heart than past attempts to induce RIPC with controlled regional ischemia.

## EXPERIMENTAL PROCEDURES

### Materials

FG-4497 was obtained from FibroGen, Inc. (San Francisco, CA, USA), and dosed at 50 mg/kg for mouse studies and 30 μM concentration for *in vitro* studies. 5 mg/ml 1-methyl-DL-tryptophan (1-MT; Sigma-Aldrich, St. Louis, MO, USA) was added to the drinking water of mice.

### Cell Culture

Immortalized mouse embryonic fibroblasts (MEFs) were made from *Egln1*+/+ and *Egln1*−/− littermates and maintained in pyruvate-free DMEM containing 10% fetal bovine serum (FBS), 1% penicillin/streptomycin (P/S). Hepa-1c1c7 mouse hepatoma cells (ATCC, Manassas, VA, USA) were grown in MEM (Corning Mediatech, Manassas, VA, USA) supplemented with 10% FBS and 1% P/S. 143B cybrid cells (Sullivan et al., 2015) were grown in DMEM supplemented with 10% FBS, 1% P/S, 1 mM sodium pyruvate, and 0.1 mg/ml uridine.

### Retroviruses

A Flag-tagged WT human *EGLN1* cDNA (Lorenzo et al., 2014) was subcloned into a pLenti vector with a CMV promoter. The H374R mutation (c.1121A→G) was made by site-directed mutagenesis. The 3XHRE luciferase reporter (Yan et al., 2007) was shuttled into a promoterless lentivirus. Lentiviruses were made by co-transfection (TransIT, Mirus Bio LLC, Madison, WI, USA) of 293TL cells with expression vectors along with the packaging constructs. Cells were infected by centrifugation in the presence of viral supernatants and polybrene.

## Mice

The *Egln1*$^{F/F}$, αMHC-Cre, Cre$^{ER}$, HSA-Cre-ER$^{T2}$ and ODD-Luc mice were previously described (Minamishima et al., 2008; Moslehi et al., 2010; Safran et al., 2006; Schuler et al., 2005). *Egln1* was deleted by treating age- and sex-matched *Egln1*$^{F/F}$ mice harboring a TAM-regulated Cre with TAM 1 mg/dose i.p.. For studies in HSA-Cre-ER$^{T2}$ mice, TAM was given daily for 5 days and mice were studied 5 days later. For studies in Cre$^{ER}$ mice, three days of TAM were given and mice were analyzed on day 4 (Minamishima et al., 2008).

## *In Vivo* Bioluminescence Imaging

*In vivo* bioluminescence imaging was done as previously described (Safran et al., 2006). Mice were given FG-4497 (i.p.) at the stated doses 2 hours before D-luciferin (150 mg/kg, i.p.).

## Ischemia-Reperfusion Injury

8–12 week old mice were anesthetized, intubated and ventilated. Left thoractotomy was performed, and the left anterior descending (LAD) artery was ligated with a 6.0 silk suture. Ischemia was confirmed by myocardial blanching and electrocardiographic (ECG) evidence of injury. Five minutes into ischemia, 50 μL of fluorescent microspheres (10 μM FluoSpheres, Molecular Probes, Eugene, OR, USA) was injected into the left ventricular cavity. The LAD ligature was released 30 minutes later and reperfusion confirmed visually by ECG. Overall survival was 70–80% at 24 hours. Mice were terminally anesthetized 24 hours after ischemia with ketamine/xylazine followed by cervical dislocation, hearts were harvested, and the ventricles were sectioned from apex to base in 2 mm sections. Sections were incubated in 2% (wt/vol) triphenyltetrazolium (TTC, Sigma) in phosphate-buffered saline at 25°C for 30 minutes. Infarct size and area at risk (AAR) was quantified from light and fluorescent micrographs of myocardial sections using Adobe Photoshop. Percent MI was calculated as the infarcted area divided by the AAR. Assessment of I/R injury in the Langendorff Model was as described (Liao et al., 2012).

Parabiosis surgeries were done as per published protocols (Wright et al., 2001). Ten days after the parabiosis operation, a subset (n=2) of parabiosed mice were used to confirm the presence of cross-circulation of blood by Evan's Blue dye injection. One mouse in each joined pair was injected with 100 μl of Evan's Blue into the retro-orbital venous plexus. Peripheral blood was collected before and 2 hours after injection. Cardiac I/R injury was performed as described above. The "recipient" partner (mouse undergoing I/R) was anesthetized and intubated per protocol while "donor" partners was anesthetized using ketamine at 80 mg/kg IP for the duration of the surgery.

## *In Vivo* Delivery of Stable Isotope Tracers

Conscious, unrestrained mice were infused with 0.19 mg/kg/minute U-$^{13}$C-TRP (Cambridge Isotopes Laboratories, Inc., Tewksbury, MA, USA) in normal saline via a central venous catheter. At 30-minute intervals, 20 μl of blood was sampled from an arterial catheter and 10 μl aliquot of plasma was snap-frozen in liquid $N_2$. After 90 min, a 50 mg/kg bolus of FG-4497 was dosed over 4 minutes. Mice were sacrificed by sodium pentobarbital (120 mg/kg), and tissues collected.

### Metabolite Extraction and Mass Spectrometry

For metabolic analyses organs were quickly dissected from euthanized mice. ~50 mg tissue sections were clamped between liquid nitrogen-cooled flat forceps, weighed, and ground. Metabolites were extracted in methanol:water:chloroform (6:3:4) by vortexing for 10 minutes at 4°C followed by centrifugation at 10,000 x *g* for 10 minutes at 4°C. Aliquots of aqueous fractions, in proportion to tissue exact mass, were dried in a refrigerated centrivap. For cell culture experiments, sample extraction were done as described (Fendt et al., 2013).

For gas chromatography mass spectrometry (GCMS) analyses, dried metabolites were derivatized and analyzed as described (Fendt et al., 2013). Reported are the dominant ions for derivatives of alpha-ketoglutarate (αKG, m/z 346), Succinate (Suc, m/z 289), and Glutamate (Glu, m/z 432). $^{13}C$ mass isotopes were quantified and corrected for natural mass isotope abundances. For liquid chromatography mass spectrometry (LC-MS) analysis of tissue metabolites, dried metabolites were resuspended in acetonitrile:methanol:formic acid (75:25:0.5 v:v:v) and samples were analyzed in positive and negative ion mode using via hydrophilic interaction liquid chromatography (HILIC) MS analyses (Avanesov et al., 2014; Townsend et al., 2013; Wang et al., 2011).

## Supplementary Material

Refer to Web version on PubMed Central for supplementary material.

## Acknowledgments

We thank Gerald Wogan, Laura Trudel, and Luiz Godoy for measuring nitrite, Rongli Lao and Souen Ngoy (Brigham and Women's Hospital, BWH) for help with cardiac I/R injury studies, Tom Cooper (Baylor College of Medicine) for the HSA-Cre$^{ER}$ mice and Lee Flippin and Michael Arend (Fibrogen) for FG- 4497. B.A.O. was supported by NIH K08 HL119355 and the Gilead Sciences Research Scholars Program in Cardiovascular Disease. JM was supported by NIH K08 HL097031, Heart Failure Society of America Research Fellowship, and the Watkins Cardiovascular Discovery Award (BWH). A.J.W. received grant support from NIH UO1 HL100402. M.G.V.H. was supported by the Broad Institute SPARC program and the Burrough's Wellcome Fund. A.J.W. was supported by a grant from the NIH. AK was funded by NIH R01 CA157971, EAH by F31 award (CA177119). W.G.K. was supported by grants from the NIH and is an HHMI Investigator. W.G.K. has a financial interest in Fibrogen, Inc., which is developing EGLN inhibitors for treating anemia and ischemic diseases.

## References

Agah R, Frenkel PA, French BA, Michael LH, Overbeek PA, Schneider MD. Gene recombination in postmitotic cells. Targeted expression of Cre recombinase provokes cardiac-restricted, site-specific rearrangement in adult ventricular muscle in vivo. J Clin Invest. 1997; 100:169–179. [PubMed: 9202069]

Agudelo LZ, Femenía T, Orhan F, Porsmyr-Palmertz M, Goiny M, Martinez-Redondo V, Correia JC, Izadi M, Bhat M, Schuppe-Koistinen I, et al. Skeletal Muscle PGC-1α1 Modulates Kynurenine Metabolism and Mediates Resilience to Stress-Induced Depression. Cell. 2014; 159:33–45. [PubMed: 25259918]

Andiné P, Lehmann A, Ellrén K, Wennberg E, Kjellmer I, Nielsen T, Hagberg H. The excitatory amino acid antagonist kynurenic acid administered after hypoxic-ischemia in neonatal rats offers neuroprotection. Neurosci Lett. 1988; 90:208–212. [PubMed: 3412643]

Avanesov AS, Ma S, Pierce KA, Yim SH, Lee BC, Clish CB, Gladyshev VN. Age- and diet-associated metabolome remodeling characterizes the aging process driven by damage accumulation. Elife. 2014; 3:e02077. [PubMed: 24843015]

Bao W, Qin P, Needle S, Erickson-Miller CL, Duffy KJ, Ariazi JL, Zhao S, Olzinski AR, Behm DJ, Pipes GCT, et al. Chronic inhibition of hypoxia-inducible factor prolyl 4-hydroxylase improves ventricular performance, remodeling, and vascularity after myocardial infarction in the rat. J Cardiovasc Pharmacol. 2010; 56:147–155. [PubMed: 20714241]

Bekeredjian R, Walton CB, MacCannell KA, Ecker J, Kruse F, Outten JT, Sutcliffe D, Gerard RD, Bruick RK, Shohet RV. Conditional HIF-1α Expression Produces a Reversible Cardiomyopathy. PLoS ONE. 2010; 5:e11693. [PubMed: 20657781]

Cai Z, Zhong H, Bosch-Marce M, Fox-Talbot K, Wang L, Wei C, Trush MA, Semenza GL. Complete loss of ischaemic preconditioning-induced cardioprotection in mice with partial deficiency of HIF-1. Cardiovascular Research. 2007; 77:463–470. [PubMed: 18006459]

Cai Z, Luo W, Zhan H, Semenza GL. Hypoxia-inducible factor 1 is required for remote ischemic preconditioning of the heart. Proceedings of the National Academy of Sciences. 2013; 110:17462–17467.

Cai Z, Manalo DJ, Wei G, Rodriguez ER, Fox-Talbot K, Lu H, Zweier JL, Semenza GL. Hearts from rodents exposed to intermittent hypoxia or erythropoietin are protected against ischemia-reperfusion injury. Circulation. 2003; 108:79–85. [PubMed: 12796124]

Coulet F, Nadaud S, Agrapart M, Soubrier F. Identification of hypoxia-response element in the human endothelial nitric-oxide synthase gene promoter. J Biol Chem. 2003; 278:46230–46240. [PubMed: 12963737]

Davies WR, Brown AJ, Watson W, McCormick LM, West NEJ, Dutka DP, Hoole SP. Remote ischemic preconditioning improves outcome at 6 years after elective percutaneous coronary intervention: the CRISP stent trial long-term follow-up. Circ Cardiovasc Interv. 2013; 6:246–251. [PubMed: 23696599]

Dickson EW, Lorbar M, Porcaro WA, Fenton RA, Reinhardt CP, Gysembergh A, Przyklenk K. Rabbit heart can be “preconditioned” via transfer of coronary effluent. Am J Physiol. 1999; 277:H2451–H2457. [PubMed: 10600868]

Eckle T, Kohler D, Lehmann R, El Kasmi KC, Eltzschig HK. Hypoxia-Inducible Factor-1 Is Central to Cardioprotection: A New Paradigm for Ischemic Preconditioning. Circulation. 2008; 118:166–175. [PubMed: 18591435]

Fendt SM, Bell EL, Keibler MA, Olenchock BA, Mayers JR, Wasylenko TM, Vokes NI, Guarente L, Vander Heiden MG, Stephanopoulos G. Reductive glutamine metabolism is a function of the α-ketoglutarate to citrate ratio in cells. Nat Commun. 2013; 4:2236. [PubMed: 23900562]

Frezza C, Zheng L, Tennant DA, Papkovsky DB, Hedley BA, Kalna G, Watson DG, Gottlieb E. Metabolic profiling of hypoxic cells revealed a catabolic signature required for cell survival. PLoS ONE. 2011; 6:e24411. [PubMed: 21912692]

Germano IM, Pitts LH, Meldrum BS, Bartkowski HM, Simon RP. Kynurenate inhibition of cell excitation decreases stroke size and deficits. Ann Neurol. 1987; 22:730–734. [PubMed: 3435082]

Gho BC, Schoemaker RG, van den Doel MA, Duncker DJ, Verdouw PD. Myocardial protection by brief ischemia in noncardiac tissue. Circulation. 1996; 94:2193–2200. [PubMed: 8901671]

Hausenloy DJ, Candilio L, Evans R, Ariti C, Jenkins DP, Kolvekar S, Knight R, Kunst G, Laing C, Nicholas J, et al. Remote Ischemic Preconditioning and Outcomes of Cardiac Surgery. N Engl J Med. 2015; 373:1408–1417. [PubMed: 26436207]

Hirsilä M, Koivunen P, Xu L, Seeley T, Kivirikko KI, Myllyharju J. Effect of desferrioxamine and metals on the hydroxylases in the oxygen sensing pathway. Faseb J. 2005; 19:1308–1310. [PubMed: 15941769]

Hölscher M, Silter M, Krull S, von Ahlen M, Hesse A, Schwartz P, Wielockx B, Breier G, Katschinski DM, Zieseniss A. Cardiomyocyte-specific prolyl-4-hydroxylase domain 2 knock out protects from acute myocardial ischemic injury. Journal of Biological Chemistry. 2011; 286:11185–11194. [PubMed: 21270129]

Huang M, Chan DA, Jia F, Xie X, Li Z, Hoyt G, Robbins RC, Chen X, Giaccia AJ, Wu JC. Short hairpin RNA interference therapy for ischemic heart disease. Circulation. 2008; 118:S226–S233. [PubMed: 18824759]

Huang Y, Hickey RP, Yeh JL, Liu D, Dadak A, Young LH, Johnson RS, Giordano FJ. Cardiac myocyte-specific HIF-1alpha deletion alters vascularization, energy availability, calcium flux, and contractility in the normoxic heart. Faseb J. 2004; 18:1138–1140. [PubMed: 15132980]

Hyvärinen J, Hassinen IE, Sormunen R, Mäki JM, Kivirikko KI, Koivunen P, Myllyharju J. Hearts of hypoxia-inducible factor prolyl 4-hydroxylase-2 hypomorphic mice show protection against acute ischemia-reperfusion injury. J Biol Chem. 2010; 285:13646–13657. [PubMed: 20185832]

Kaelin WG, Ratcliffe PJ. Oxygen sensing by metazoans: the central role of the HIF hydroxylase pathway. Molecular Cell. 2008; 30:393–402. [PubMed: 18498744]

Kalakech H, Tamareille S, Pons S, Godin-Ribuot D, Carmeliet P, Furber A, Martin V, Berdeaux A, Ghaleb B, Prunier F. Role of hypoxia inducible factor-1α in remote limb ischemic preconditioning. Journal of Molecular and Cellular Cardiology. 2013; 65:98–104. [PubMed: 24140799]

Kloner RA, Shook T, Przyklenk K, Davis VG, Junio L, Matthews RV, Burstein S, Gibson M, Poole WK, Cannon CP. Previous angina alters inhospital outcome in TIMI 4. A clinical correlate to preconditioning? Circulation. 1995; 91:37–45. [PubMed: 7805217]

Kottenberg E, Thielmann M, Bergmann L, Heine T, Jakob H, Heusch G, Peters J. Protection by remote ischemic preconditioning during coronary artery bypass graft surgery with isoflurane but not propofol - a clinical trial. Acta Anaesthesiol Scand. 2012; 56:30–38. [PubMed: 22103808]

Kottenberg E, Musiolik J, Thielmann M, Jakob H, Peters J, Heusch G. Interference of propofol with signal transducer and activator of transcription 5 activation and cardioprotection by remote ischemic preconditioning during coronary artery bypass grafting. J Thorac Cardiovasc Surg. 2014; 147:376–382. [PubMed: 23465551]

Kummitha CM, Kalhan SC, Saidel GM, Lai N. Relating tissue/organ energy expenditure to metabolic fluxes in mouse and human: experimental data integrated with mathematical modeling. Physiol Rep. 2014; 2

Ladroue C, Carcenac R, Leporrier M, Gad S, Le Hello C, Galateau-Salle F, Feunteun J, Pouysségur J, Richard S, Gardie B. PHD2 mutation and congenital erythrocytosis with paraganglioma. N Engl J Med. 2008; 359:2685–2692. [PubMed: 19092153]

Laitala A, Aro E, Walkinshaw G, Mäki JM, Rossi M, Heikkilä M, Savolainen ER, Arend M, Kivirikko KI, Koivunen P, et al. Transmembrane prolyl 4-hydroxylase is a fourth prolyl 4-hydroxylase regulating EPO production and erythropoiesis. Blood. 2012; 120:3336–3344. [PubMed: 22955912]

Lewis GD, Wei R, Liu E, Yang E, Shi X, Martinovic M, Farrell L, Asnani A, Cyrille M, Ramanathan A, et al. Metabolite profiling of blood from individuals undergoing planned myocardial infarction reveals early markers of myocardial injury. J Clin Invest. 2008; 118:3503–3512. [PubMed: 18769631]

Liao R, Podesser BK, Lim CC. The continuing evolution of the Langendorff and ejecting murine heart: new advances in cardiac phenotyping. AJP: Heart and Circulatory Physiology. 2012; 303:H156–H167. [PubMed: 22636675]

Lorenzo FR, Huff C, Myllymäki M, Olenchock B, Swierczek S, Tashi T, Gordeuk V, Wuren T, Ri-Li G, McClain DA, et al. A genetic mechanism for Tibetan high-altitude adaptation. Nat Genet. 2014; 46:951–956. [PubMed: 25129147]

Metallo CM, Gameiro PA, Bell EL, Mattaini KR, Yang J, Hiller K, Jewell CM, Johnson ZR, Irvine DJ, Guarente L, et al. Reductive glutamine metabolism by IDH1 mediates lipogenesis under hypoxia. Nature. 2012; 481:380–384. [PubMed: 22101433]

Meybohm P, Bein B, Brosteanu O, Cremer J, Gruenewald M, Stoppe C, Coburn M, Schaelte G, Böning A, Niemann B, et al. A Multicenter Trial of Remote Ischemic Preconditioning for Heart Surgery. N Engl J Med. 2015; 373:1397–1407. [PubMed: 26436208]

Minamishima YA, Moslehi J, Bardeesy N, Cullen D, Bronson RT, Kaelin WG. Somatic inactivation of the PHD2 prolyl hydroxylase causes polycythemia and congestive heart failure. Blood. 2008; 111:3236–3244. [PubMed: 18096761]

Moslehi J, Minamishima YA, Shi J, Neuberg D, Charytan DM, Padera RF, Signoretti S, Liao R, Kaelin WG. Loss of Hypoxia-Inducible Factor Prolyl Hydroxylase Activity in Cardiomyocytes Phenocopies Ischemic Cardiomyopathy. Circulation. 2010; 122:1004–1016. [PubMed: 20733101]

Murry CE, Jennings RB, Reimer KA. Preconditioning with ischemia: a delay of lethal cell injury in ischemic myocardium. Circulation. 1986; 74:1124–1136. [PubMed: 3769170]

Natarajan R, Salloum FN, Fisher BJ, Kukreja RC, Fowler AA. Hypoxia inducible factor-1 activation by prolyl 4-hydroxylase-2 gene silencing attenuates myocardial ischemia reperfusion injury. Circulation Research. 2006; 98:133–140. [PubMed: 16306444]

Nwogu JI, Geenen D, Bean M, Brenner MC, Huang X, Buttrick PM. Inhibition of collagen synthesis with prolyl 4-hydroxylase inhibitor improves left ventricular function and alters the pattern of left ventricular dilatation after myocardial infarction. Circulation. 2001; 104:2216–2221. [PubMed: 11684634]

Przyklenk K. Special article: reduction of myocardial infarct size with ischemic "conditioning": physiologic and technical considerations. Anesth Analg. 2013; 117:891–901. [PubMed: 23960036]

Przyklenk K, Bauer B, Ovize M, Kloner RA, Whittaker P. Regional ischemic "preconditioning" protects remote virgin myocardium from subsequent sustained coronary occlusion. Circulation. 1993; 87:893–899. [PubMed: 7680290]

Pundir M, Arora S, Kaur T, Singh R, Singh AP. Effect of modulating the allosteric sites of N-methyl-D-aspartate receptors in ischemia-reperfusion induced acute kidney injury. J Surg Res. 2013; 183:668–677. [PubMed: 23498342]

Ristagno G, Fries M, Brunelli L, Fumagalli F, Bagnati R, Russo I, Staszewsky L, Masson S, Li Volti G, Zappalà A, et al. Early kynurenine pathway activation following cardiac arrest in rats, pigs, and humans. Resuscitation. 2013; 84:1604–1610. [PubMed: 23774325]

Robinson A, Keely S, Karhausen J, Gerich ME, Furuta GT, Colgan SP. Mucosal protection by hypoxia-inducible factor prolyl hydroxylase inhibition. Gastroenterology. 2008; 134:145–155. [PubMed: 18166352]

Ronkainen VP, Tuomainen T, Huusko J, Laidinen S, Malinen M, Palvimo JJ, Ylä-Herttuala S, Vuolteenaho O, Tavi P. Hypoxia-inducible factor 1-induced G protein-coupled receptor 35 expression is an early marker of progressive cardiac remodelling. Cardiovascular Research. 2014; 101:69–77. [PubMed: 24095869]

Safran M, Kim WY, O'Connell F, Flippin L, Günzler V, Horner JW, Depinho RA, Kaelin WG. Mouse model for noninvasive imaging of HIF prolyl hydroxylase activity: assessment of an oral agent that stimulates erythropoietin production. Proc Natl Acad Sci USa. 2006; 103:105–110. [PubMed: 16373502]

Schuler M, Ali F, Metzger E, Chambon P, Metzger D. Temporally controlled targeted somatic mutagenesis in skeletal muscles of the mouse. Genesis. 2005; 41:165–170. [PubMed: 15789425]

Stoll B, Hüssinger D. Functional hepatocyte heterogeneity. Vascular 2-oxoglutarate is almost exclusively taken up by perivenous, glutamine-synthetase-containing hepatocytes. Eur J Biochem. 1989; 181:709–716. [PubMed: 2567236]

Sullivan LB, Gui DY, Hosios AM, Bush LN, Freinkman E, Vander Heiden MG. Supporting Aspartate Biosynthesis Is an Essential Function of Respiration in Proliferating Cells. Cell. 2015; 162:552–563. [PubMed: 26232225]

Thielmann M, Kottenberg E, Kleinbongard P, Wendt D, Gedik N, Pasa S, Price V, Tsagakis K, Neuhäuser M, Peters J, et al. Cardioprotective and prognostic effects of remote ischaemic preconditioning in patients undergoing coronary artery bypass surgery: a single-centre randomised, double-blind, controlled trial. Lancet. 2013; 382:597–604. [PubMed: 23953384]

Townsend MK, Clish CB, Kraft P, Wu C, Souza AL, Deik AA, Tworoger SS, Wolpin BM. Reproducibility of metabolomic profiles among men and women in 2 large cohort studies. Clin Chem. 2013; 59:1657–1667. [PubMed: 23897902]

Vogler M, Zieseniss A, Hesse AR, Levent E, Tiburcy M, Heinze E, Burzlaff N, Schley G, Eckardt K-U, Willam C, et al. Pre- and post-conditional inhibition of prolyl-4-hydroxylase domain enzymes protects the heart from an ischemic insult. Pflugers Arch - Eur J Physiol. 2015

Wang TJ, Larson MG, Vasan RS, Cheng S, Rhee EP, McCabe E, Lewis GD, Fox CS, Jacques PF, Fernandez C, et al. Metabolite profiles and the risk of developing diabetes. Nat Med. 2011; 17:448–453. [PubMed: 21423183]

Wise DR, Ward PS, Shay JES, Cross JR, Gruber JJ, Sachdeva UM, Platt JM, DeMatteo RG, Simon MC, Thompson CB. Hypoxia promotes isocitrate dehydrogenase-dependent carboxylation of α-

ketoglutarate to citrate to support cell growth and viability. Proceedings of the National Academy of Sciences. 2011; 108:19611–19616.

Wright DE, Wagers AJ, Gulati AP, Johnson FL, Weissman IL. Physiological migration of hematopoietic stem and progenitor cells. Science. 2001; 294:1933–1936. [PubMed: 11729320]

Wu CC, Hsu CW, Chen CD, Yu CJ, Chang KP, Tai DI, Liu HP, Su WH, Chang YS, Yu JS. Candidate serological biomarkers for cancer identified from the secretomes of 23 cancer cell lines and the human protein atlas. Mol Cell Proteomics. 2010; 9:1100–1117. [PubMed: 20124221]

Yan Q, Bartz S, Mao M, Li L, Kaelin WG. The Hypoxia-Inducible Factor 2 N-Terminal and C-Terminal Transactivation Domains Cooperate To Promote Renal Tumorigenesis In Vivo. Molecular and Cellular Biology. 2007; 27:2092–2102. [PubMed: 17220275]

Zwilling D, Huang SY, Sathyasaikumar KV, Notarangelo FM, Guidetti P, Wu HQ, Lee J, Truong J, Andrews-Zwilling Y, Hsieh EW, et al. Kynurenine 3-monooxygenase inhibition in blood ameliorates neurodegeneration. Cell. 2011; 145:863–874. [PubMed: 21640374]

## HIGHLIGHTS

- Inhibition of EglN1 locally or at a distance protects the heart against I/R injury
- Remote ischemic protection after EglN1 loss is mediated by a humoral factor
- Diversion of the EglN co-substrate αKG stimulates hepatic kynurenic acid production

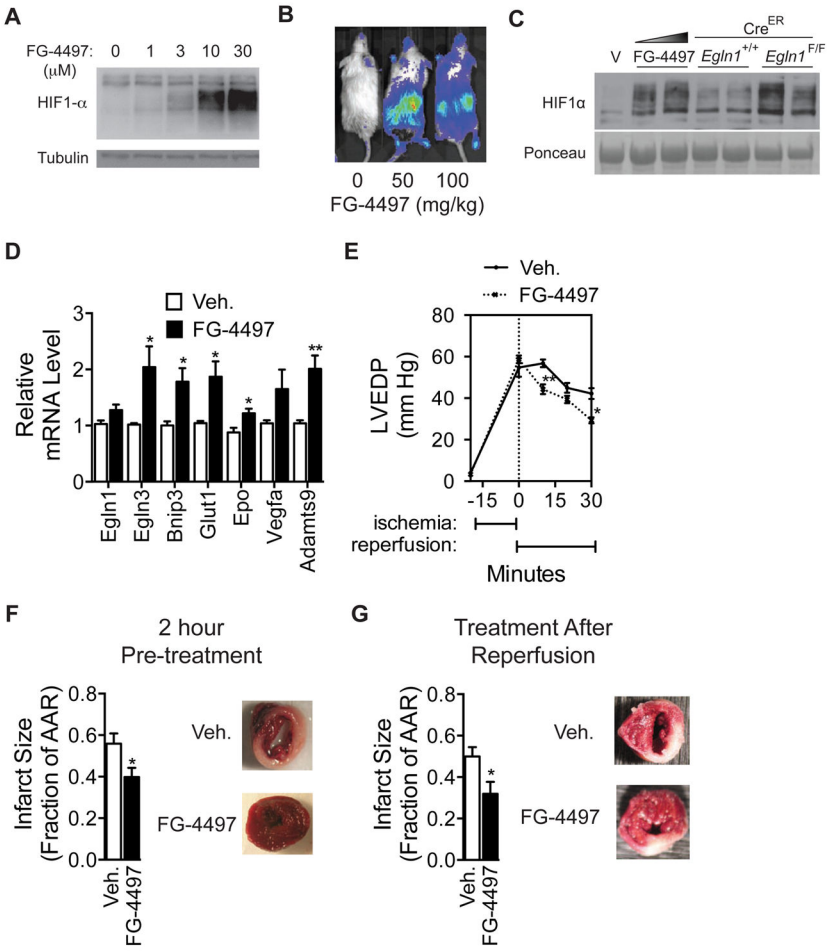


**Figure 1. Acute Systemic Inhibition of Egln Protects Against Cardiac I/R Injury**

(A) Representative immunoblots of HL-1 cardiomyocytes treated with FG-4497 for 6 hours.

(B) Bioluminescent images of representative mice expressing a HIF-luciferase fusion protein 3 hours after being given intravenous (i.v.) FG-4497.

(C) HIF1α protein levels in the hearts of mice given 50 or 100 mg/kg FG-4497 i.v., as indicated by the triangle, or after systemic *Egln1* genetic deletion. *Egln1*$^{F/F}$; Cre-ER and *Egln1*$^{+/+}$; Cre-ER mice were given TAM for 5 days before sacrifice.

(D) Real-time PCR assays of mRNAs in the heart 3 hours after i.p. administration of 50 mg/kg FG-4497 (n=5) or vehicle (n=4). Data shown are mean fold changes ± SEM. *p<0.05, **p<0.01, Student's *t*-test, FG-4497 versus vehicle (Veh.).

(E) LVEDP in Langendorff assays of global I/R injury. Mice were given 50 mg/kg FG-4497 i.v. or Veh. 2 hours before cardiectomy. Data shown are mean pressures ± SEM, n = 8 in each group. *p<0.05, **p<0.01, Student's *t*-test.

(F) MI size after cardiac I/R injury in mice given 50 mg/kg FG-4497 i.p. or Veh. two hours before *in vivo* cardiac I/R injury. Data are normalized to the Area-at-Risk (AAR). Data shown are means ± SEM, n = 8 FG-4497 and n = 7 vehicle. *p<0.05, Student's *t*-test. Representative photographs of TTC-stained hearts are shown.

(G) MI size relative to AAR in mice given 50 mg/kg FG-4497 i.p. or Veh. at the time of LAD reperfusion. Data shown are means ± SEM, n = 6 FG-4497 and n = 5 vehicle. *$p<0.05$, Student's *t*-test. Representative photographs of TTC-stained hearts are shown.

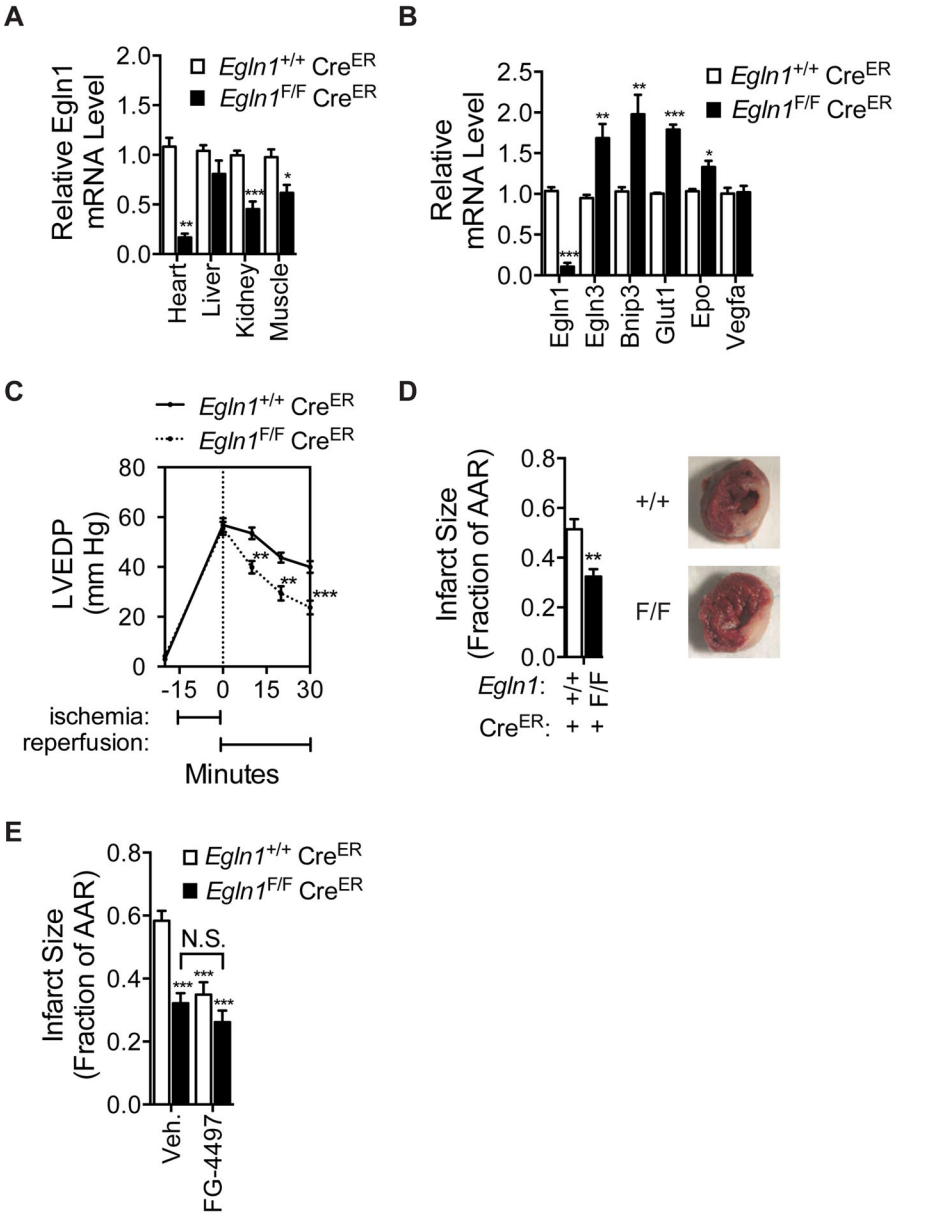


**Figure 2. Acute Systemic Deletion of *Egln1* Protects Against Cardiac I/R Injury**

(A) Real-time PCR assays of *Egln1* mRNA in tissues from *Egln1*$^{F/F}$; Cre$^{ER}$ and *Egln1*$^{+/+}$; Cre$^{ER}$ mice. Mice were given TAM for 3 days and sacrificed 3 days later. Data shown are mean fold changes ± SEM, n = 4 in each group. *p<0.05, **p<0.01, ***p<0.01, Student's *t*-test, difference in mRNA levels between *Egln1*$^{F/F}$; Cre$^{ER}$ and *Egln1*$^{+/+}$; Cre$^{ER}$ mice.

(B) Real-time PCR assays of select HIF-responsive mRNAs in the hearts from TAM-treated *Egln1*$^{F/F}$; Cre$^{ER}$ and *Egln1*$^{+/+}$; Cre$^{ER}$ mice. Data shown are mean fold changes ± SEM, n = 4 in each group. *p<0.05, **p<0.01, ***p<0.01, Student's *t*-test, difference in mRNA levels between *Egln1*$^{F/F}$; Cre$^{ER}$ and *Egln1*$^{+/+}$; Cre$^{ER}$ mice.

(C) LVEDP in Langendorff assays of global I/R injury. Mice were given TAM as in (A) before cardiectomy. Data shown are mean pressures ± SEM, n = 6 in each group. **p<0.01, ***p<0.01, Student's *t*-test.

(D) MI size relative to AAR after *in vivo* cardiac I/R injury in TAM-treated *Egln1*$^{F/F}$; Cre$^{ER}$ and *Egln1*$^{+/+}$; Cre$^{ER}$ mice. Data shown are means ± SEM, n = 10 mice per group. **p<0.01, Student's *t*-test.

(E) MI size after cardiac I/R injury in TAM-treated *Egln1*$^{F/F}$; Cre$^{ER}$ and *Egln1*$^{+/+}$; Cre$^{ER}$ mice, pre-treated with 50 mg/kg FG-4497 i.v. or Veh. two hours before cardiac I/R injury. Data shown are means ± SEM, n = 8 FG-4497 and n = 7 vehicle groups. ***p<0.001, Student's *t*-test, differences MI sizes compared to Veh.-treated *Egln1*$^{+/+}$; Cre$^{ER}$ mice. See Figure S1.

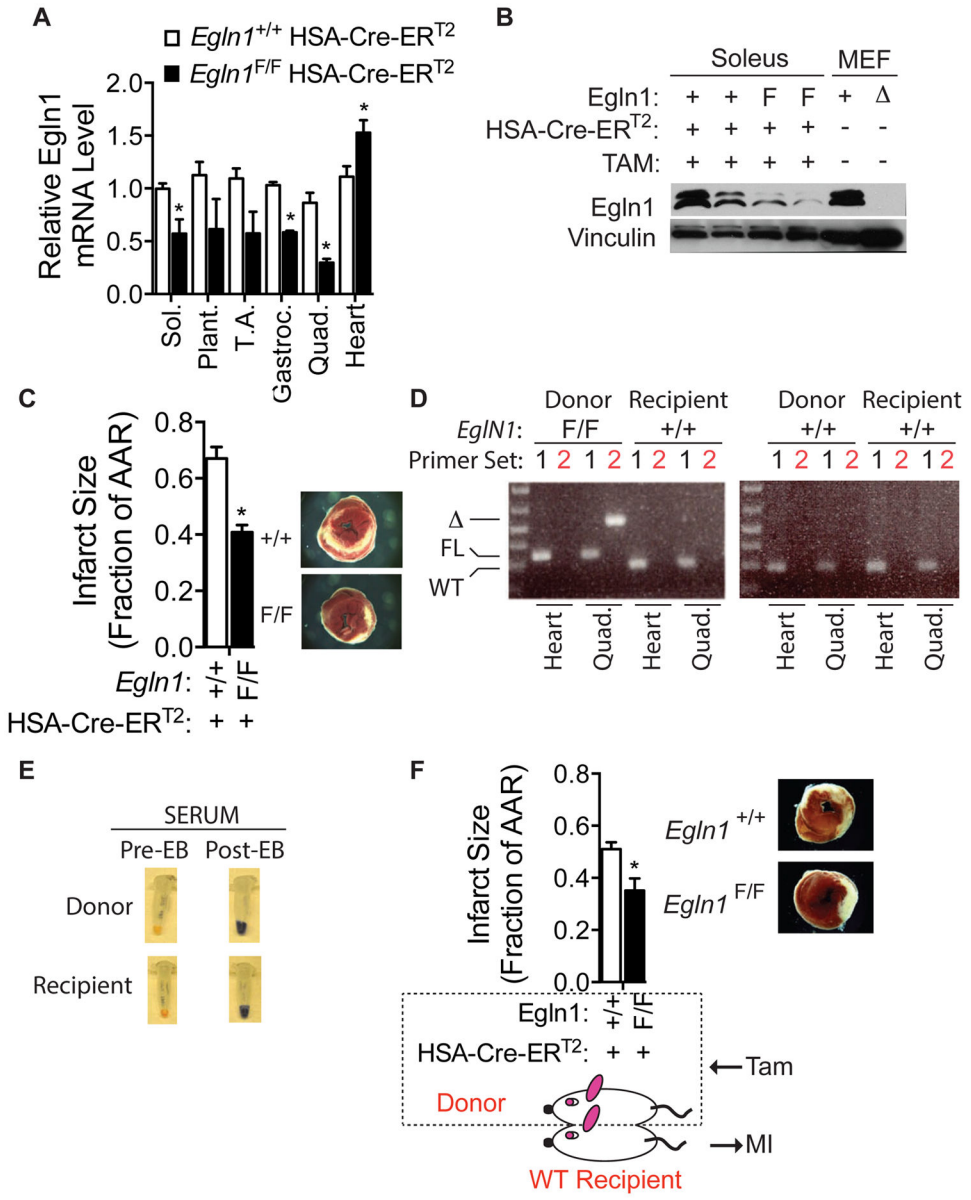


**Figure 3. Skeletal Muscle *Egln1* Deletion Confers Remote Cardioprotection via a Circulating Factor**

(A) Real-time PCR assays of *Egln1* mRNA levels in indicated tissues from TAM-treated *Egln1*$^{F/F}$; HSA-Cre-ER$^{T2}$ and *Egln1*$^{+/+}$; HSA-Cre-ER$^{T2}$ mice. Abbreviations: soleus (Sol.), plantaris (Plant.), tibialis anterior (T.A.), gastrocnemius (Gastroc.), quadriceps (Quad.). Data shown are mean fold changes ± SEM. *p<0.05, Student's *t*-test, differences in mRNA levels in *Egln1*$^{F/F}$; HSA-Cre-ER$^{T2}$ mice compared to *Egln1*$^{+/+}$; HSA-Cre-ER$^{T2}$ mice.

(B) Immunoblots of extracts from Sol. muscle of TAM-treated *Egln1*$^{F/F}$; HSA-Cre-ER$^{T2}$ and *Egln1*$^{+/+}$; HSA-Cre-ER$^{T2}$ mice. Egln1 WT (+) and knockout (Δ) MEFs were included for comparison.

(C) MI size after cardiac I/R injury in TAM-treated *Egln1*$^{F/F}$; HSA-Cre-ER$^{T2}$ and *Egln1*$^{+/+}$; HSA-Cre-ER$^{T2}$ mice. Data shown are means ± SEM, n = 6 mice per group. *p<0.05, Student's *t*-test. Representative photographs of TTC-stained hearts are shown.

(D) PCR genotyping of the heart and quadriceps (Quad) of 'donor' and 'recipient' parabiosis mice. Donor mice were TAM-treated *Egln1*$^{F/F}$; HSA-Cre-ER$^{T2}$ and *Egln1*$^{+/+}$; HSA-Cre-ER$^{T2}$ mice, as indicated. *Egln1* primer set 1 amplifies WT and floxed (FL) alleles, and primer set 2 amplifies the deleted allele (Δ).

(E) Representative serum samples from parabiosis 'donor' and 'recipient' mice before and 2 hours after i.v. injection of Evan's blue (EB) dye.

(F) MI size after cardiac I/R injury in WT mice that were surgically conjoined to either a TAM-treated *Egln1*$^{F/F}$; HSA-Cre-ER$^{T2}$ mouse or a TAM-treated *Egln1*$^{+/+}$; HSA-Cre-ER$^{T2}$ mouse. WT 'recipient' mice were subjected to cardiac I/R and MI size quantified 24 hours later. Data shown are means ± SEM, n = 6 *Egln1*$^{F/F}$; HSA-Cre-ER$^{T2}$ and n = 8 *Egln1*$^{+/+}$; HSA-Cre-ER$^{T2}$ mice. *p<0.05, Student's *t*-test, difference in MI size in WT mice conjoined to *Egln1*$^{F/F}$; HSA-Cre-ER$^{T2}$ mice vs. WT mice conjoined to *Egln1*$^{+/+}$; HSA-Cre-ER$^{T2}$ mice. Representative photographs of TTC-stained hearts are shown.

See also Figure S2.

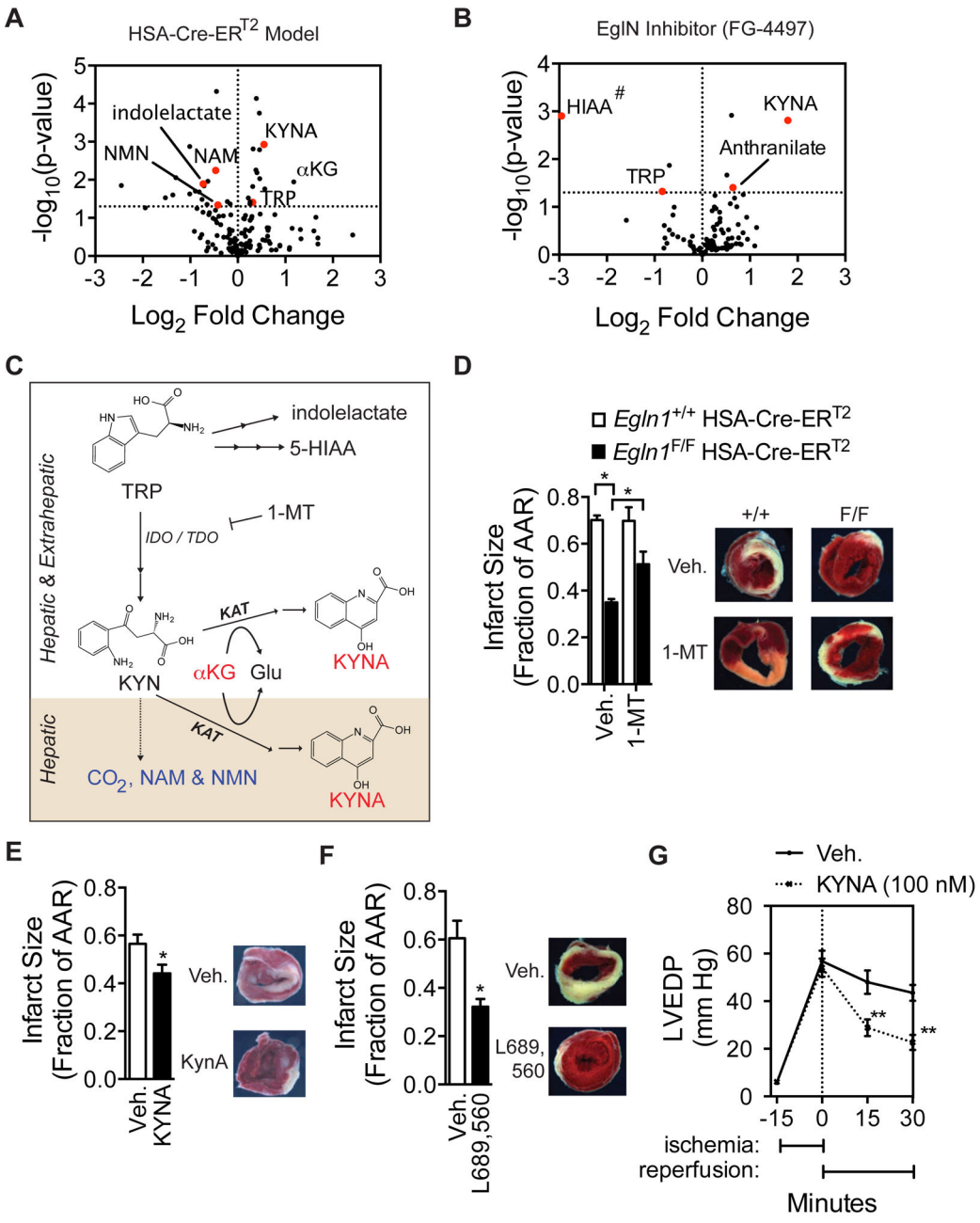


**Figure 4. The TRP Metabolite Kynurenic Acid is Necessary and Sufficient for Remote Cardiac I/R Protection**

(A) Volcano plot depicting fold change and statistical significance in ion counts for serum metabolites in TAM-treated *Egln1*$^{F/F}$; HSA-Cre-ER$^{T2}$ mice compared to *Egln1*$^{+/+}$; HSA-Cre-ER$^{T2}$ mice. Abbreviations: KYNA – kynurenic acid; αKG – alpha-ketoglutarate; TRP – tryptophan; NAM – niacinamide; NMN – n-methyl-nicotinamide. Metabolites above the dotted line are those that differ with $p<0.05$ (Student's *t*-test, n=6). TRP metabolites are shown in red.

(B) Volcano plot depicting fold change and statistical significance of serum metabolites in mice given FG-4497 compared to Veh-treated animals. Labeled are the TRP metabolites

KYNA, Anthranilate, and 5-hydroxyindoleacetic acid (HIAA). Metabolites above the dotted line are those that differ with $p<0.05$ (Student's *t*-test, n=3). #HIAA was undetectable in serum of mice given FG-4497. TRP metabolites are shown in red.

(C) Diagram of TRP metabolism, including the rate-limiting pyrolase IDO, present in peripheral tissues, TDO, present in the liver, the IDO/TDO inhibitor 1-methyltryptophan (1-MT), and the regulated kynurenine (KYN) aminotransferases (KAT). The direct product of KYN transamination by KATs, 4-(2-aminophenyl)-2,3-dioxobutanoate (not shown), is non-enzymatically dehydrated to produce KYNA.

(D) MI size after cardiac I/R injury in TAM-treated *Egln1*$^{F/F}$; HSA-Cre-ER$^{T2}$ and *Egln1*$^{+/+}$; HSA-Cre-ER$^{T2}$ mice given the IDO/TDO inhibitor 1-methyltryptophan (1-MT) or vehicle (Veh.) for 3 days before I/R. Data shown are means ± SEM, n = 5 *Egln1*$^{F/F}$; HSA-Cre-ER$^{T2}$ vehicle, n = 5 *Egln1*$^{F/F}$; HSA-Cre-ER$^{T2}$ 1-MT, n = 3 *Egln1*$^{+/+}$; HSA-Cre-ER$^{T2}$ vehicle, n = 4 *Egln1*$^{+/+}$; HSA-Cre-ER$^{T2}$ 1-MT. * $p<0.05$, Student's *t*-test, for designated comparisons.

(E) MI size after cardiac I/R injury in WT mice pretreated with 100 ng KYNA or Veh. i.p. 2-hr before and 2 hr after *in vivo* cardiac I/R. Data shown are means ± SEM, n = 16 vehicle, n=14 KYNA. *$p<0.05$, Student's *t*-test.

(F) MI size after cardiac I/R injury in WT mice given 40 mg/kg KYNA mimetic L689,560 or Veh. i.p. immediately before I/R injury. Data shown are means ± SEM, n = 3 per group. *$p<0.05$, Student's *t*-test.

(G) LVEDP in Langendorff assays after global I/R injury, with or without 100 nM KYNA present in the perfusate. Data shown are mean pressures ± SEM, n = 10 KYNA group and n = 9 control group. **$p<0.01$, Student's *t*-test.

See also Figure S3.

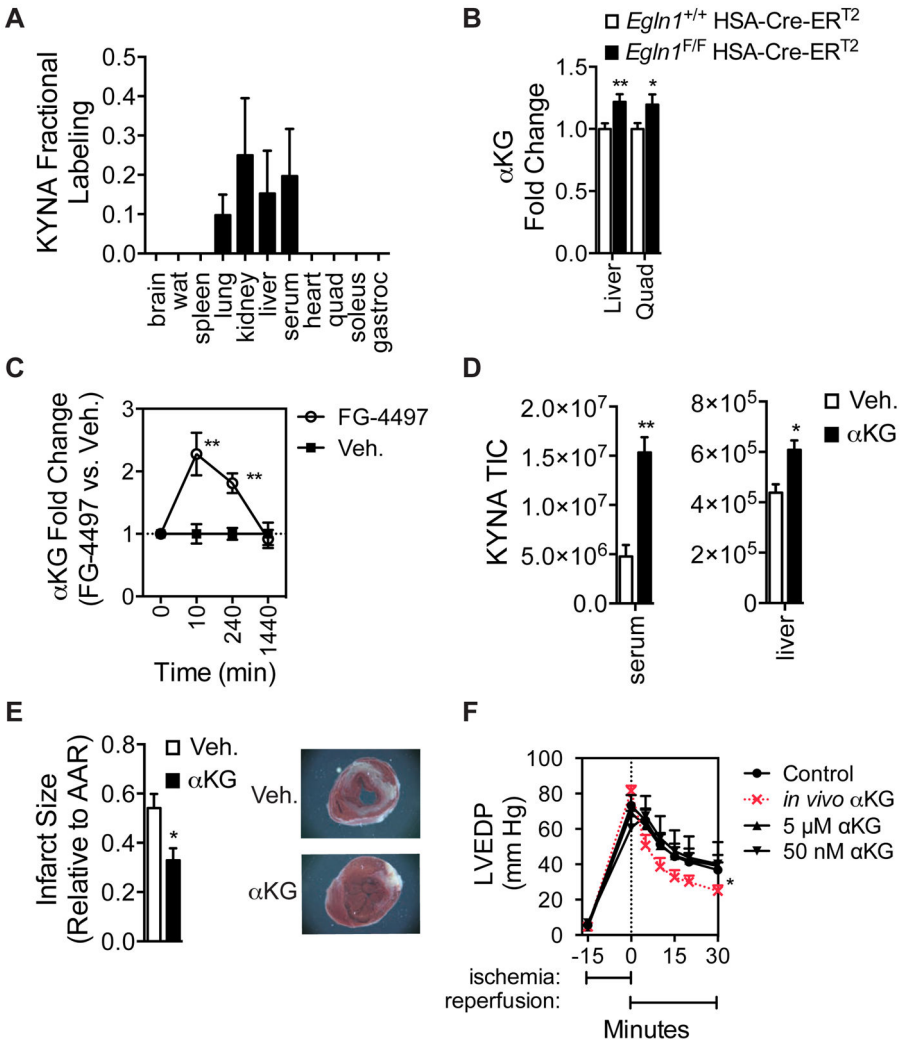


**Figure 5. Altered Systemic αKG Metabolism in *Egln1*$^{F/F}$ HSA-Cre-ER$^{T2}$ Mice Leads to Cardioprotection Through KYNA**

(A) Fractional labeling of U-$^{13}$C-KYNA in tissues. WT mice were infused with U-$^{13}$C-TRP until serum isotopic equilibrium was reached and then given 50 mg/kg FG-4497 i.v. Tissues were harvest 30 minutes later. Shown are mean enrichment ± SEM, n = 2.

(B) αKG levels in liver and quadriceps (Quad) of TAM-treated *Egln1*$^{F/F}$; HSA-Cre-ER$^{T2}$ and *Egln1*$^{+/+}$; HSA-Cre-ER$^{T2}$ mice. Shown are mean fold change ± SEM, n = 23, **p<0.01, *p<0.05, Student's *t*-test, comparison between EglN$^{f/f}$; HSA-Cre-ER$^{T2}$ and *Egln1*$^{+/+}$; HSA-Cre-ER$^{T2}$ mice.

(C) Hepatic αKG levels in WT mice given 50 mg/kg FG-4497 i.v. or Veh. Shown are mean fold change ± SEM, n = 5. **p<0.01 Student's *t*-test.

(D) KYNA levels in serum and liver of mice given 1 mg/kg αKG or Veh. i.p. Shown are mean total ion counts (TIC) quantified by LC-MS, ± SEM, n = 3. *p<0.05, **p<0.01 Student's *t*-test.

(E) MI size in WT mice treated as in (D) 2 hours before cardiac I/R injury. Data shown are means ± SEM, n = 4 vehicle, n=6 αKG. *p<0.05, Student's *t*-test. Representative photographs of TTC-stained hearts are shown.
(F) LVEDP in Langendorff assays after global I/R injury with or without αKG present in the perfusate at the indicated concentrations. One group of mice was pretreated with 1 mg/kg αKG i.p. 45 minutes before sacrifice. Data shown are mean pressures ± SEM. *p<0.05, Student's *t*-test, for differences at 30 minutes compared to control.
See also Figure S4.

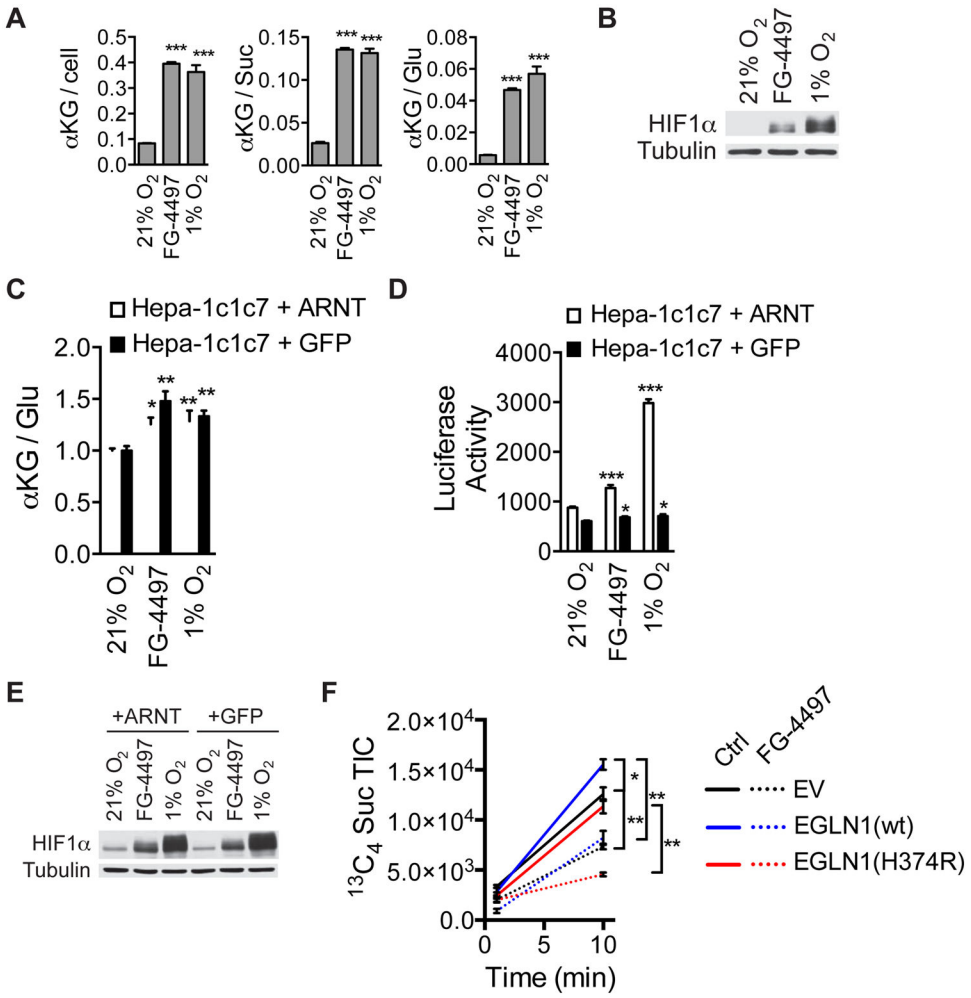


**Figure 6. Egln Activity Regulates αKG Levels in a HIF-independent Manner**

(A) αKG levels in WT MEFs given FG-4497 or cultured under 1% $O_2$ conditions for 24 hours. Data are normalized to internal standard and cell number, succinate TIC (Suc), or glutamate TIC (Glu). ***p<0.001, Student's *t*-test, differences compared to untreated MEFs grown in 21% $O_2$. Shown are mean ± SEM, n = 3.

(B) Immunoblots of WT MEFs treated as in (A).

(C) αKG / Glutamate ratios of Hepa-1c1c7 ARNT−/− cells stably expressing exogenous ARNT or GFP and treated with FG-4497 or 1% $O_2$ for 24 hours. *p<0.05, **p<0.01, Student's *t*-test, differences compared to untreated MEFs grown in 21% $O_2$. Shown are mean ± SEM, n =8.

(D) Firefly luciferase activity in Hepa-1c1c7 expressing exogenous ARNT or GFP, as in (C), and harboring a HIF-responsive firefly luciferase reporter. Cells were treated with FG-4497 or 1% $O_2$ for 24 hours as indicated. Shown are mean ± SEM, n =8. *p<0.05, ***p<0.001, Student's *t*-test, differences relative to untreated cells grown in 21% $O_2$.

(E) Immunoblots of cells used in (C) and (D).

(F) Total ion counts of $^{13}C_4$-succinate (Suc) in WT 143B cells at indicated time points after addition of U-$^{13}$C-dimethyl-αKG. Shown are mean ± SEM, n = 4. *p<0.05 and **p<0.01, Student's *t*-test, comparisons designated.
See also Figure S5.